

# Evaluating the Performance of a Carbon-Epoxy Capillary Cathode and Carbon Fiber Cathode in a Sealed-Tube Vircator Under UHV Conditions

Evan Rocha, Patrick M. Kelly, Jonathan M. Parson, Curtis F. Lynn, James C. Dickens, Andreas A. Neuber, John J. Mankowski, Tal Queller, Joseph Gleizer, and Yakov E. Krasik.

**Abstract**—This paper evaluates the performance of a bimodal carbon fiber cathode and a carbon-epoxy multicapillary cathode operating within a reflex-triode sealed-tube virtual cathode oscillator (vircator). The experimental results reveal that both cathodes exhibit similar emission behavior, although with some significant operational differences. An eight-stage 84-J pulse-forming network-based Marx generator serves to drive both cathodes at 250 kV and 3–4 kA with a  $\sim 70$ -ns pulsewidth. Both cathodes undergo conditioning over 10 000 pulses to determine gas evolution as well as electrical changes over time. Gas evolution of both cathodes is observed using a residual gas analyzer to determine individual gas constituents. A comparison of diode voltage, diode current, RF output, and outgassing data for both cathodes during vircator operation over 10 000 pulses is presented to quantify cathode performance in a sealed-tube vircator. Changes in cathode surface morphology, from virgin to postmortem, are discussed. Data for various anode–cathode gap distances, from 3 to 15 mm, are presented. The evolution of voltage and current inputs to the vircator is discussed.

**Index Terms**—Cathodes, electron emission, electron tubes, high power microwave generator.

## I. INTRODUCTION

WHILE there is a general interest in large-area cathodes, this paper is focused on their performance within a virtual cathode oscillator (vircator). A variety of different cathodes were previously tested, including carbon fiber (CF) cathodes with varying fiber lengths and striplike cathodes, which consist of a single strip of CF capillaries [1], [2]. The dominant electron emission processes are not always well

defined and may vary from one cathode type to another. One source of emission relies on surface flashover along the base of the emitter tips while another may be due to explosive emission localized at the tips. In general, surface flashover depends on the rise time of the accelerating voltage and exhibits faster turn-ON over explosive emission, while explosive emission suffers from increased gas desorption from the cathode. In the case of surface flashover, plasma formation starts to occur with electric fields as low as 10 kV/cm [2].

Previously, polymer velvet cathodes were used as an electron source. This type of cathode contains randomly oriented tips on the cathode surface. However, the major drawbacks to this type of cathode are the short lifetime that lasts only from one hundred to a few thousand pulses as well as the continued outgassing of the nonvacuum compatible velvet [3], [4]. To counteract the low lifetime of the velvet cathode, an all-metal cathode was designed, which performed as well if not better than the velvet cathode [5]. While the high outgassing rate of the velvet cathode gave it a major disadvantage, when compared with a graphite cathode, the application of a velvet cathode in microwave devices showed larger peak power and width of the microwave pulse [6].

A cathode combining the positive properties of metal and velvet cathode types, low outgassing and quick turn-ON ( $\leq 10$  kV/cm), is the bimodal CF cathode. When compared with the velvet cathode, CF cathodes show almost constant diode impedance, whereas velvet cathodes do not [7], [8]. Optical measurements and scanning electron microscope (SEM) imaging strongly indicate that the dominant electron source mechanism of this cathode is explosive electron emission [3], [8]–[10]. This type of cathode can be conditioned over 10 000 pulses with a current density of several tens of amperes per square centimeter to improve the overall outgassing of the cathode while keeping the electrical properties consistent [11].

Recently, carbon-epoxy multicapillary (CEM) cathodes have shown to efficiently produce large-area electron beams [1]. In this case, the flashover plasma formation occurs at an electric field of around 15 kV/cm. Also, this cathode shows no degradation over thousands of pulses in emission properties, all but excluding explosive emission as the

Manuscript received October 14, 2014; revised April 3, 2015; accepted May 19, 2015. Date of publication July 21, 2015; date of current version August 7, 2015.

E. Rocha, P. M. Kelly, J. M. Parson, C. F. Lynn, J. C. Dickens, A. A. Neuber, and J. J. Mankowski are with the Center for Pulsed Power and Power Electronics, Department of Electrical and Computer Engineering, Texas Tech University, Lubbock, TX 79409 USA (e-mail: evan.rocha@ttu.edu; pmk0024.kelly@ttu.edu; jonathan.m.parson@ttu.edu; curtislynn@ttu.edu; james.dickens@ttu.edu; andreas.neuber@ttu.edu; john.mankowski@ttu.edu).

T. Queller, J. Z. Gleizer, and Y. E. Krasik are with the Department of Physics, Technion–Israel Institute of Technology, Haifa 3200003, Israel (e-mail: quellertal@gmail.com; gleizer@physics.technion.ac.il; finkrasik@physics.technion.ac.il).

Color versions of one or more of the figures in this paper are available online at <http://ieeexplore.ieee.org>.

Digital Object Identifier 10.1109/TPS.2015.2439680

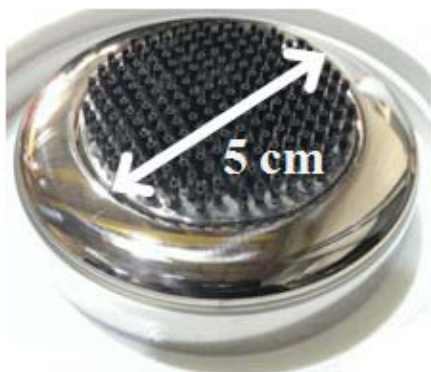


Fig. 1. CEM cathode.

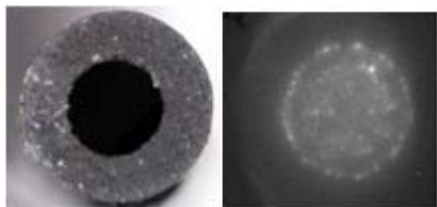


Fig. 2. Single capillary (left) and light emission from the CEM cathode (right). The frame duration is 20 ns [2].

dominant mechanism [2]. There has been no evidence of gap closure from this type of cathode at current densities up to  $5 \text{ kA/cm}^2$ , due to plasma formation occurring inside the carbon-epoxy capillaries. Furthermore, it was demonstrated that the cathode has a uniform electron beam that can be produced repeatedly [1].

## II. EXPERIMENTAL SETUP

### A. Carbon-Epoxy Multicapillary Cathode

Two different cathodes have been evaluated. The CEM cathode consists of 208 CF capillaries uniformly arranged on a stainless steel substrate, as shown in Fig. 1.

The carbon-epoxy capillaries are adhered to the stainless steel substrate by Durabond 954 [2]. This epoxy is a metallic composite high expansion adhesive for high-temperature bonding. The length of the capillaries decreases toward the periphery of the cathode to minimize the field enhancement at the edge of the cathode. Each individual capillary is 7 mm in length, with a 1.5-mm outer diameter and a 0.7-mm inner diameter. The total surface area of the CEM cathode is  $14.7 \text{ cm}^2$ . Fig. 2 shows an individual capillary on the left and observed light emission during a single pulse from a capillary on the right. As can be observed, the light emission is uniform and indicative of surface flashover occurring within the capillary tubes. This causes the cathode to turn ON quickly due to the fact that surface flashover occurs at lower electric fields, within an average range of 15–30 kV/cm [2]. Furthermore, the plasma formation from the CEM cathode is a result of surface flashover occurring on the tips of the capillary tubes [12].

### B. Carbon Fiber Cathode

The bimodal CF cathode has two million CFs pyrolytically bonded to a POCO graphite substrate that was developed by

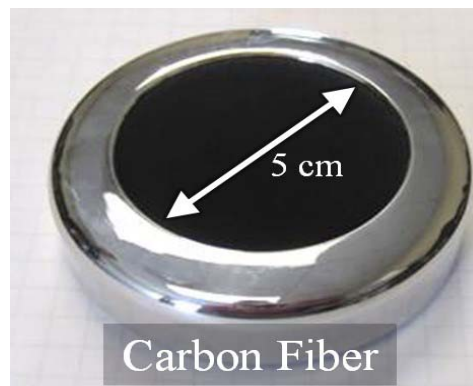


Fig. 3. CF cathode [9].

the Air Force Research Laboratory and produced by Energy Science Laboratories, Inc. Bimodal operation of the cathode refers to the fact that there are fibers of two different lengths. Of the two million fibers,  $\sim 1.8$  million fibers are 1.5-mm long and  $\sim 200\,000$  fibers are 2-mm long. Each individual fiber is about  $5 \mu\text{m}$  in diameter [9]. They are randomly distributed and arranged throughout the entire surface of the cathode. The CF cathode has a slightly larger surface area of  $20 \text{ cm}^2$ . In order to mitigate the field enhancement on the edge of the CF cathode, a Rogowski-profile field-shaping ring is used, as shown in Fig. 3.

As mentioned in Section I, this type of cathode is believed to be characterized by the formation of the explosive emission plasma at a background pressure of  $10^{-9}$  torr [9]. The application of the accelerating pulse leads to the appearance of a large electric field enhancement ( $> 10^7 \text{ V/cm}$ ) at the tips of the CFs and to large current densities at those locations. High current densities cause rapid joule heating of the fibers, resulting in the tips of the fibers exploding and formation of explosive emission plasma. Both cathodes operate under ultrahigh vacuum (UHV) conditions and were baked out at  $300 \text{ }^\circ\text{C}$  for 72 h prior to operation. Due to their critical influence on the results, each component was extensively cleaned as described in [11]. It is important to note that a residual gas analyzer (RGA) is attached to the vircator and baked along with the entire vacuum section to achieve background pressures around  $10^{-9}$  torr, with surfaces mostly free of adsorbed gas layers.

### C. Sealed-Tube Reflex-Triode Vircator and Marx Generator

Both cathodes were extensively tested within a sealed-tube reflex-triode vircator. With its tunability and compactness, the vircator has distinct advantages over other High Power Microwaves (HPM) sources. It may be noted, however, that vircator tube efficiency is typically limited to less than 10% [13]. Fig. 5 shows a cutaway view of the reflex-triode vircator in which both a bimodal CF cathode and a CEM cathode were compared. The cathode is attached to a linear actuator and three-axis port aligner allowing it to be adjusted accordingly. In order to reduce field enhancements on the cathode, a field-shaping ring is placed around the cathode. The details on the field-shaping ring are described in [14].

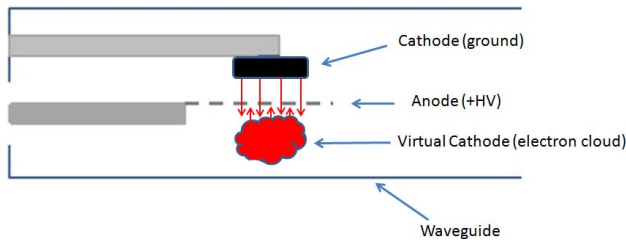


Fig. 4. Operation of the reflex-triode vircator.

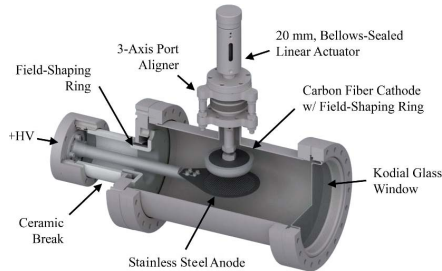


Fig. 5. Cutaway view of the reflex-triode vircator.

The reflex-triode vircator operates by pulsing the anode positive high-voltage, establishes a high electric field across the anode–cathode (A–K) gap, and accelerates electrons from the cathode to the anode. The anode is a titanium mesh with 70% effective transparency such that a majority of the electrons pass through the anode screen, where they form an oscillating electron cloud beneath the anode surface. This electron cloud is termed a virtual cathode, which oscillates at a frequency according to its electron density. These oscillations, in conjunction with electrons reflexing through the anode screen, generate microwave radiation. This is graphically represented in Fig. 4.

In order to drive the vircator, an eight-stage pulse-forming network (PFN)-based Marx generator is used. A four-stage Rayleigh PFN configuration was implemented to create the required high voltage pulse. Spark gaps in a pressurized tube were used as the switching mechanism between each stage. The gap distance for each spark gap was set using a highpot tester. The initial gap was set to break down at 14 kV in air. Each consecutive gap was increased by 2-kV increments with the final gap breaking down at 28 kV. The pressure in the tube was set to ensure no prebreakdown occurred during charging. The entire Marx generator was placed in oil to prevent breakdown between stages.

A 50-kV charging supply rated for 4 kW charges the Marx for 42 ms. Four 2.1-nF capacitors in parallel rated at 50 kV form each PFN stage of the Marx, with a total capacitance of 67.2 nF and stored energy of 84 J. Output from the Marx generation may vary anywhere from 150 to 400 kV at a 50-kV charge, dependent on the A–K gap distance. The Marx generator has roughly a 60- $\Omega$  output impedance with a full-width at half-maximum of approximately 70 ns.

#### D. Diagnostics

Multiple factors were considered to fully observe the performance of the cathode. The outgassing characteristics of the cathodes were measured to ensure that the outgassing produced by the cathode is low enough to maintain UHV conditions inside the vircator. A bakeable RGA from Extorr is used to detect different gas constituents inside the vircator after each pulse. The control unit was removed during firing to prevent damage during operation. Directly after a single pulse, the control unit was placed on the RGA to run a mass spectrum sweep ranging from 1 to 120 amu.

To read accurate voltage, current, and microwave data, careful placements and considerations must be made. A capacitive voltage divider is placed at the feedthrough to the vircator to read the voltage that is being supplied directly to the anode. The feedthrough is calibrated to ensure the magnitude of the voltage waveforms is measured correctly. A Rogowski coil is placed on the ground return path directly after the vircator. The Rogowski coil measures the  $di/dt$  of the current, which is then later integrated. A wideband receiving horn antenna is used that covers all microwave frequencies in the region of interest.

### III. EXPERIMENTAL RESULTS

The following procedure remained consistent throughout the entire conditioning process. Outgassing characteristics for each cathode were measured over 10000 pulses. Outgassing data were recorded after each individual shot for shots 1–100, when the outgassing conditioning curve is steepest. Following this, RGA measurements were taken in a logarithmic fashion for shots 250, 500, 750, 1000, 1500, 2500, 5000, 7500, and 10000. Intermediate shots were taken at a 0.5-Hz repetition rate for 500 pulse bursts. The vircator was allowed to recover UHV conditions by means of a small 20-L/s ion pump after each burst. During each burst, the ion pump was left on, ensuring that the vircator maintained vacuum. The pressures would reach as high as  $10^{-5}$  torr during each burst and would take several minutes to recover to a minimum of  $10^{-9}$  torr. During each single pulse, the ion pump was left OFF to ensure accurate outgassing data were collected. A 50-kV charging voltage and 8-mm A–K gap were kept consistent throughout the conditioning process for the CEM cathode. A 9-mm A–K gap was used for the CF cathode. The average voltage being supplied to the vircator is  $\sim 200$  kV with  $\sim 3$  kA of current initially. This results in a current density of  $\sim 150$  A/cm<sup>2</sup>. However, for the CEM cathode, the voltage increased to 250 kV with a 4-kA increase due to the change in impedance of the diode. This could be due to the fact that several capillaries fell out during the operation.

#### A. Gas Evolution

Individual gas constituents were measured for both cathodes with the use of the RGA. Fig. 6 shows gas evolution for four primary gas constituents observed during the vircator operation, in order of prevalence: hydrogen and its isotopes, nitrogen, methane, and argon. There is a minimal reduction in

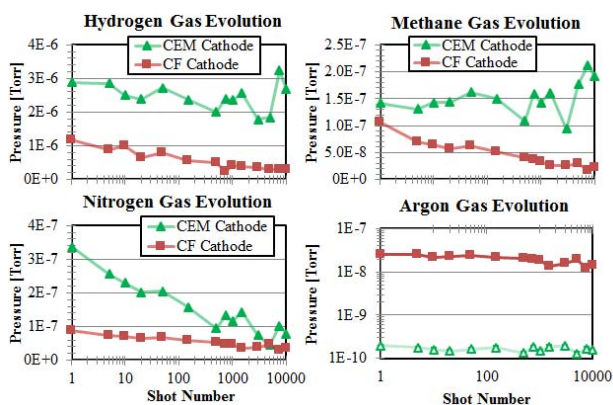


Fig. 6. Gas evolution for 10000 shots. Note the differing pressure scales.

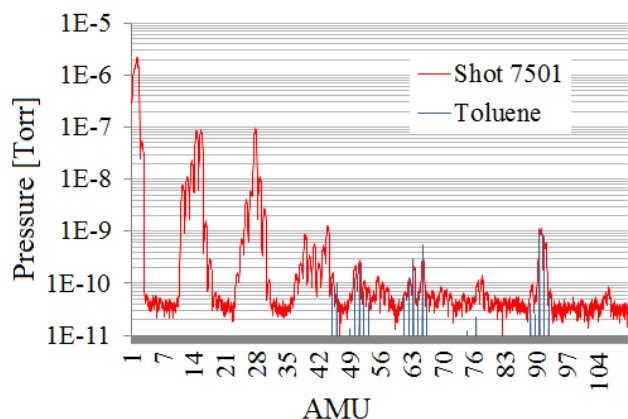


Fig. 7. Mass spectrum sweep of CEM cathode at shot 7501. Toluene cracking pattern is indicated in blue.

outgassing for the first 45 pulses, except for nitrogen, for the CEM cathode.

It is important to note that nitrogen shows a dramatic decrease compared with other gases. The amount of methane desorbed, however, increases throughout the conditioning curve. This is problematic, as most ion pumps are inefficient at pumping methane relative to the other desorbed gas constituents. The comparative lack of argon in the CEM cathode gas data may be attributed to the fact that the CF cathode was exposed to a 90% argon/10% oxygen microwave plasma cleaning, whereas the CEM cathode was not.

It is interesting to note when observing the mass spectrum for the CEM cathode over a wide range of masses, the presences of long-chain hydrocarbons are measured after long bursts. These are not typically seen in CF cathodes stringently cleaned by UHV conditions. As observed in Fig. 7, the evidence of toluene is shown based on the cracking pattern [15]. This is probably due to prolonged excessive heating from either the CF tubes or the bonding adhesive, owing to the fact that it was only observed after long bursts, which contributes to excessive heating of the cathode. Toluene is a common material used in adhesives, as well as cleaning agents, which could have been used in the manufacturing of the capillaries [16].

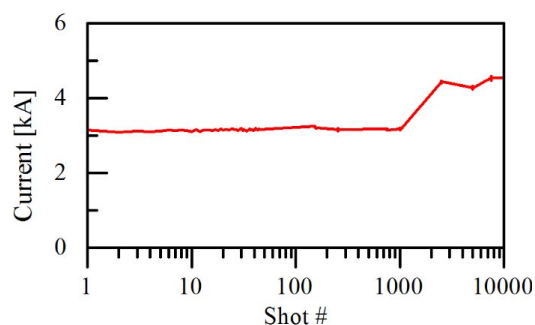


Fig. 8. Peak current as a function of shot number for the CEM cathode.

### B. Input Voltage and Current

Interestingly, a drastic increase in current was observed after approximately 2500 pulses, an increase which remained throughout the conditioning process. After this increase, the current plateaued again (see Fig. 8). However, previous studies carried out at moderate vacuum ( $10^{-5}$  torr) show that even after around 4000 pulses, the current and voltage did not change [2]. This drastic change in behavior is thought to be due to the *postmortem* observation that some of the capillaries had fallen out of place due to the high temperatures that the cathode reached during bakeout and operation. The increased current amplitude is then simply due to the effectively reduced A–K gap size.

Compared with the bimodal CF cathode, the electron emission from the CEM cathode is almost simultaneous with the voltage pulse that agrees with similar experiments [1]. In the case of explosive emission plasma formation, this effect can most likely be attributed to electrons that are first sourced via field emission, that is, a large electric field (larger than is needed for surface flashover) has to be established to overcome the work function potential barrier. Only when the field emission current is high enough and flows for a sufficiently long period of time, explosive emission will occur and enhance the electron emission process. However, one can also suppose that this type of the cathode is characterized by flashover plasma formation along the fiber surface [4]. In this case, a long rise in the current is related to strong dependence of the amount of plasma spots and their radial and axial expansions on rise time and amplitude of the accelerating voltage [2].

In the case of the CF-based cathode, the plasma is formed at the surface of numerous fibers, which has been shown in [17] and [18]. The thermal expansion of this plasma toward the anode and in the transverse directions leads to a gradual increase in the amplitude of electron current due to a decrease in the effective A–K gap and due to an increase in the plasma emitting surface as well.

In the case of the CEM-based cathode, the plasma formation occurs at the surface of a finite number of capillaries placed at a rather significant distance (a few millimeters) from each other. The threshold of the formation of this plasma is around of a few kilovolts per centimeter. In this case, the plasma of a single capillary expands toward the anode and in transverse direction. However, opposite to the case of the

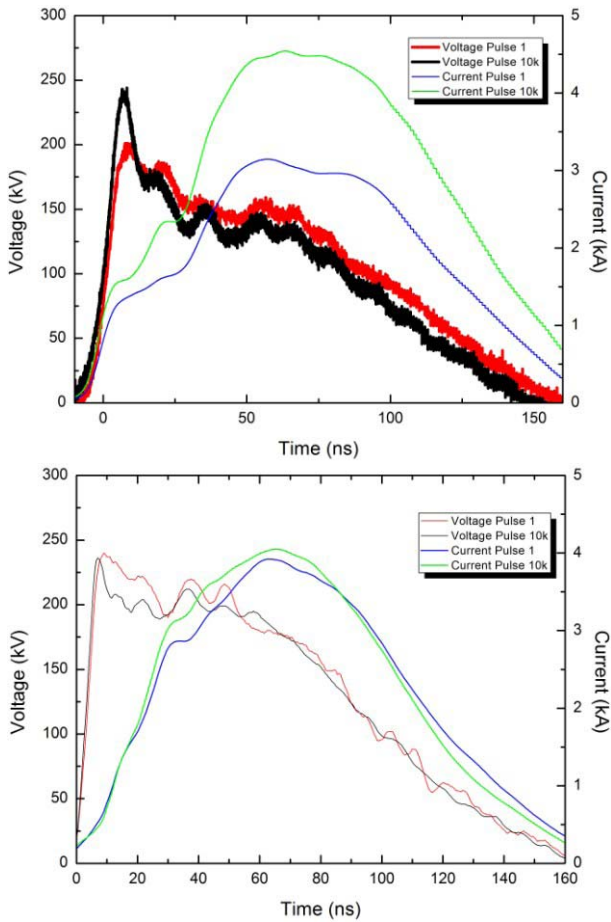


Fig. 9. Voltage and current waveforms for shots 1 and 10000. Top: CEM cathode. Bottom: bimodal CF cathode. Bimodal CF data are from [9].

CF-based cathodes, the density of these single plasma sources decreases significantly faster toward the anode than in the case of CF cathodes. Thus, one obtains on the one hand an increase in the emitting area due to transverse plasma expansion and on the other hand a decrease in the plasma density of the plasma. The latter leads to the limitation in the rise time of the emitting current density observed in Fig. 9.

### C. RF Output

The RF outputs of both cathodes are similar. Even with the incurred damage, the CEM cathode still showed roughly the same amount of RF output. The input voltages and current from both cathodes are also very similar. Both cathodes exhibit repeatability of the RF electric field. However, the overall RF electric field from each of the cathodes varies by about 10 kV/m. The CF cathode produces electric fields up to  $\sim 31$  kV/m, measured 2 m away [9]. Under the same operating conditions, the CEM cathode produced fields only up to 20 kV/m, again, measured at a distance of 2 m. The current and voltage for the CF cathode to achieve a maximum RF output were  $\sim 260$  kV and 4.3 kA, respectively. The CEM cathode generated a maximum RF output at similar voltages of  $\sim 250$  kV, but at lower currents of 3.1 kA. This is

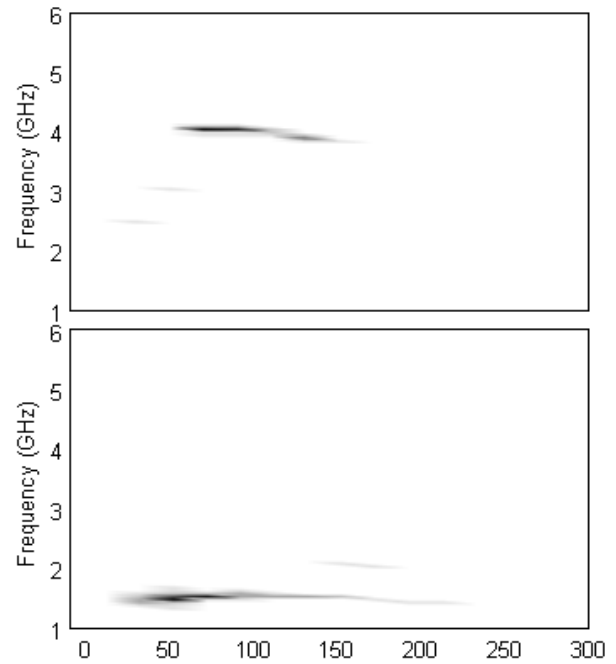


Fig. 10. Frequency of operation for a vircator using a CEM cathode. Top: 8-mm A-K gap. Bottom: 16-mm A-K gap.

most likely due to a difference in diode impedance between the CEM and CF cathode vircators, and could be accounted for by tuning the A-K gap. Opening the A-K gap caused an increase in the voltage, and subsequently, the frequency lowered from 4.1 GHz at a 8-mm gap down to the resonant frequency of the cavity, which is about 1.5 GHz at 16 mm, as observed from Fig. 10 [14].

### D. Imaging

Several images of both cathodes were taken before and after conditioning to investigate degradation of the cathode. An SEM was used to take images of the CF cathode to observe the individual fibers of the cathode. SEM imaging showed evidence of explosive electron emission due to degradation of the tips of the individual fibers from high current densities [9].

The CEM cathode was too large and too heavy to fit into the available SEM setup. Hence, the CEM cathode was optically imaged both before and after as well. Certain capillaries were already cracked prior to operation. Fig. 11 shows that after 10000 pulses, the capillary cracks grew larger. This could be caused by the rapid heating and cooling of the cathode during the operation, which would affect the overall lifetime of the cathode itself. Furthermore, it appears that some of the adhesive, which uses a stainless steel base, on the sides of the individual capillaries has started to peel off showing signs of wear on the capillaries.

## IV. DISCUSSION

Overall, the outgassing rate of the CEM cathode is very high compared with the CF cathode. This is of concern when working with any sealed HPM tube. While the plasma

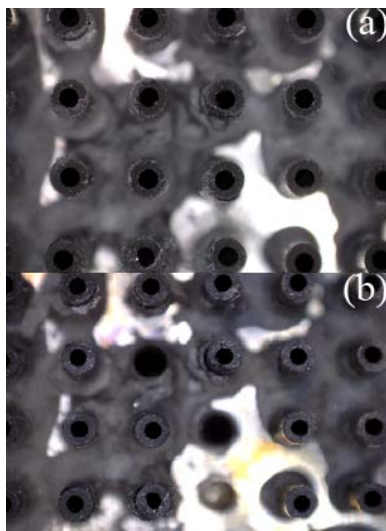


Fig. 11. Optical image of the CEM cathode. (a) Virgin capillaries. (b) Capillaries after 10000 pulses. Note the missing capillaries in (b).

formation apparently aids in electron emission turn-ON, it is considered detrimental to stable operation, and may lead to premature A–K gap closure for longer pulse lengths. In addition, the significant outgassing makes operation of the vircator at high repetition rates impossible with the tested CEM. Note that a 500-Hz repetition rate was previously reported for a vircator with the CF cathode [19].

If one assumes that the root cause for the increased outgassing lies in the utilized bonding material, one might consider repeating testing with an improved bonding method for the CEM cathode. A different adhesive may solve the problem of some of the capillaries falling out during the operation. A carbon-based paste and base with similar thermal coefficients of expansion should reduce the mechanical fatigue of the cathode. Furthermore, reducing the size of the CEM cathode could possibly improve the performance of the cathode. By reducing the cathode size, the current density will increase, which may result in a higher RF output power of the vircator with the CEM cathode.

## V. CONCLUSION

The major electrical characteristics and the RF output of two large-area cathodes, capillary and fiber based (CEM and CF), were shown to be similar. However, the CEM cathode resulted in a lower RF output power. Future upgrades in materials utilized in the construction of the CEM may improve the performance to levels comparable with the CF.

## REFERENCES

- [1] T. Queller, J. Z. Gleizer, and Y. E. Krasik, "High-current long-duration uniform electron beam generation in a diode with multicapillary carbon-epoxy cathode," *J. Appl. Phys.*, vol. 114, no. 12, p. 123303, 2013.
- [2] J. Z. Gleizer *et al.*, "High-current carbon-epoxy capillary cathode," *J. Appl. Phys.*, vol. 112, no. 2, p. 023303, 2012.
- [3] D. Shiffler *et al.*, "Review of cold cathode research at the Air Force Research Laboratory," *IEEE Trans. Plasma Sci.*, vol. 36, no. 3, pp. 718–728, Jun. 2008.
- [4] D. Shiffler *et al.*, "Comparison of velvet- and cesium iodide-coated carbon fiber cathodes," *IEEE Trans. Plasma Sci.*, vol. 29, no. 3, pp. 445–451, Jun. 2001.
- [5] Y. J. Chen, A. A. Neuber, J. Mankowski, J. C. Dickens, M. Kristiansen, and R. Gale, "Design and optimization of a compact, repetitive, high-power microwave system," *Rev. Sci. Instrum.*, vol. 76, no. 10, p. 104703, 2005.
- [6] R. Menon *et al.*, "High power microwave generation from coaxial virtual cathode oscillator using graphite and velvet cathodes," *J. Appl. Phys.*, vol. 107, no. 9, p. 093301, 2010.
- [7] J. Yang, T. Shu, and H. Wang, "Improved long-term electrical stability of pulsed high-power diodes using dense carbon fiber velvet cathodes," *Phys. Plasmas*, vol. 19, no. 7, p. 072119, 2012.
- [8] A. Roy, A. Patel, R. Menon, A. Sharma, D. P. Chakravarthy, and D. S. Patil, "Emission properties of explosive field emission cathodes," *Phys. Plasmas*, vol. 18, no. 10, p. 103108, 2011.
- [9] J. M. Parson, C. F. Lynn, J. J. Mankowski, A. A. Neuber, and J. C. Dickens, "Emission behavior of three conditioned carbon fiber cathode types in UHV-sealed tubes at 200 A/cm<sup>2</sup>," *IEEE Trans. Plasma Sci.*, vol. 42, no. 12, pp. 3982–3988, Dec. 2014.
- [10] J. M. Parson, J. J. Mankowski, J. C. Dickens, and A. A. Neuber, "Imaging of explosive emission cathode and anode plasma in a vacuum-sealed vircator high-power microwave source at 250 A/cm<sup>2</sup>," *IEEE Trans. Plasma Sci.*, vol. 42, no. 10, pp. 2592–2593, Oct. 2014.
- [11] J. M. Parson, C. F. Lynn, J. J. Mankowski, M. Kristiansen, A. A. Neuber, and J. C. Dickens, "Conditioning of carbon fiber cathodes in UHV-sealed tubes at 200 A/cm<sup>2</sup>," *IEEE Trans. Plasma Sci.*, vol. 42, no. 8, pp. 2007–2014, Aug. 2014.
- [12] T. Queller, J. Z. Gleizer, Y. E. Krasik, V. A. Bernshtam, and U. Dai, "High-current carbon-epoxy capillary cathode," *IEEE Trans. Plasma Sci.*, vol. 42, no. 5, pp. 1224–1236, May 2014.
- [13] R. J. Barker and E. Schamiloglu, Eds., *High-Power Microwave Sources and Technologies*. New York, NY, USA: Wiley, 2001, p. 13.
- [14] C. F. Lynn *et al.*, "Frequency tuning a reflex triode vircator," in *Proc. Int. Power Modulator High Voltage Conf.*, Santa Fe, NM, USA, 2014.
- [15] P. J. Linstrom and W. G. Mallard. (2001). *NIST Chemistry Webbook; NIST Standard Reference Database No. 69*. [Online]. Available: <http://webbook.nist.gov>
- [16] (Jul. 2012). *Toluene*. [Online]. Available: <http://www.epa.gov>, accessed May 16, 2014.
- [17] Y. E. Krasik *et al.*, "Emission properties of different cathodes at  $E \leq 10^5$  V/cm," *J. Appl. Phys.*, vol. 89, no. 4, p. 2379, 2001.
- [18] Y. E. Krasik *et al.*, "Characterization of the plasma on dielectric fiber (velvet) cathodes," *J. Appl. Phys.*, vol. 98, no. 9, p. 093308, 2005.
- [19] J. M. Parson *et al.*, "A frequency stable vacuum-sealed tube high-power microwave vircator operated at 500 Hz," *IEEE Electron Device Lett.*, vol. 36, no. 5, pp. 508–510, May 2015.

Authors' photographs and biographies not available at the time of publication.